Supplementary Information

Alkali Metal-Mediated Interfacial Charge Redistribution Toward Near-Optimal Water Oxidation

Ungsoo Kim,[‡a] Sangjin Lee,[‡b] Nam Khen Oh,[‡a] Jihyung Seo,[a] Ji Hoo Cha,[a] Junghyun Lee,[a] Seong-hun Lee,[c] Tae Joo Shin,[cd] Jeong Min Baik,*[ef] Young-Kyu Han,*[b] and Hyesung Park*[ad]

[a]Department of Materials Science and Engineering, Low Dimensional Carbon Materials Center, Ulsan National Institute of Science and Technology, Ulsan 44919, Republic of Korea

[b]Department of Energy and Materials Engineering, Dongguk University-Seoul, Seoul 04620, Republic of Korea

[c]UNIST Central Research Facilities, Ulsan National Institute of Science and Technology (UNIST), Ulsan 44919, Republic of Korea

[d]Graduate School of Semiconductor Materials and Devices Engineering, Ulsan National Institute of Science and Technology (UNIST), Ulsan 44919, Republic of Korea

[e]School of Advanced Materials Science and Engineering, Sungkyunkwan University (SKKU), Suwon 16419, Republic of Korea

[f]KIST-SKKU Carbon-Neutral Research Center, Sungkyunkwan University (SKKU), Suwon 16419, Republic of Korea

*Corresponding authors

E-mail address: hspark@unist.ac.kr (H. Park), ykenergy@dongguk.edu (Y.-K. Han) jbaik97@skku.edu (J. M. Baik)

‡These authors contributed equally to this work.

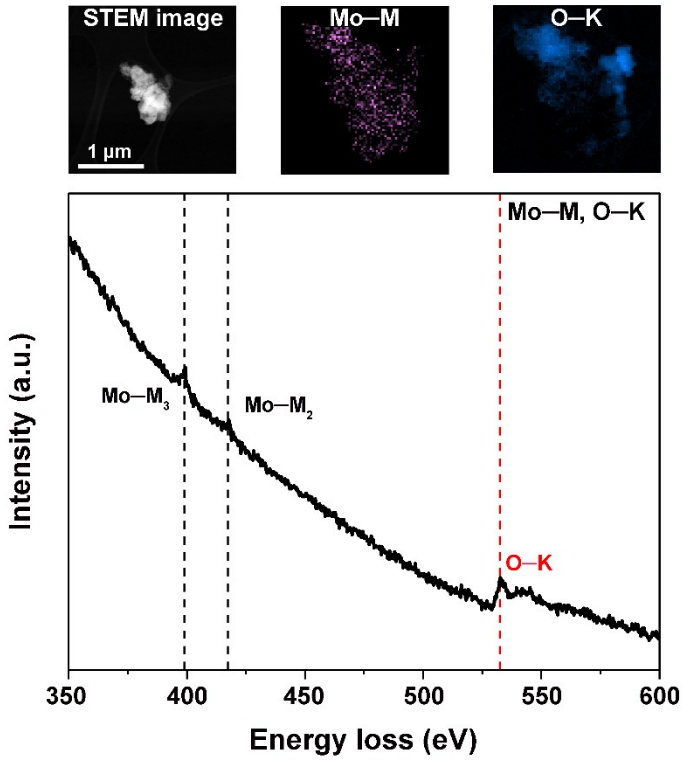

Fig. S1 EELS spectrum and corresponding chemical map of Mo–M and O–K edges for LSC/LMO.

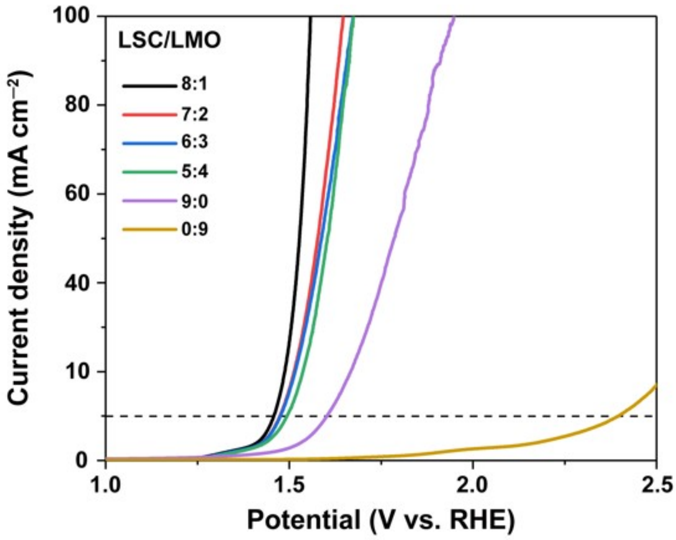

Fig. S2 OER polarization curves of LSC/LMO with different weight ratios.

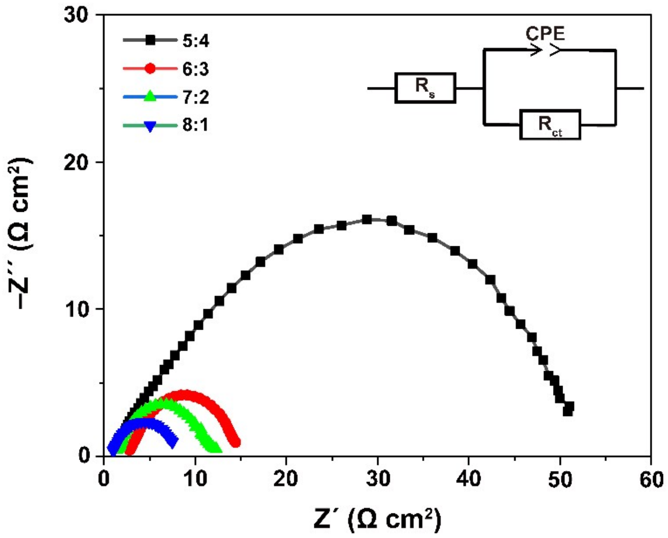

Fig. S3 Nyquist plots of LSC/LMO for OER with various weight ratios. Inset: Equivalent electrical circuit model used for fitting the Nyquist complex-plane impedance plot.

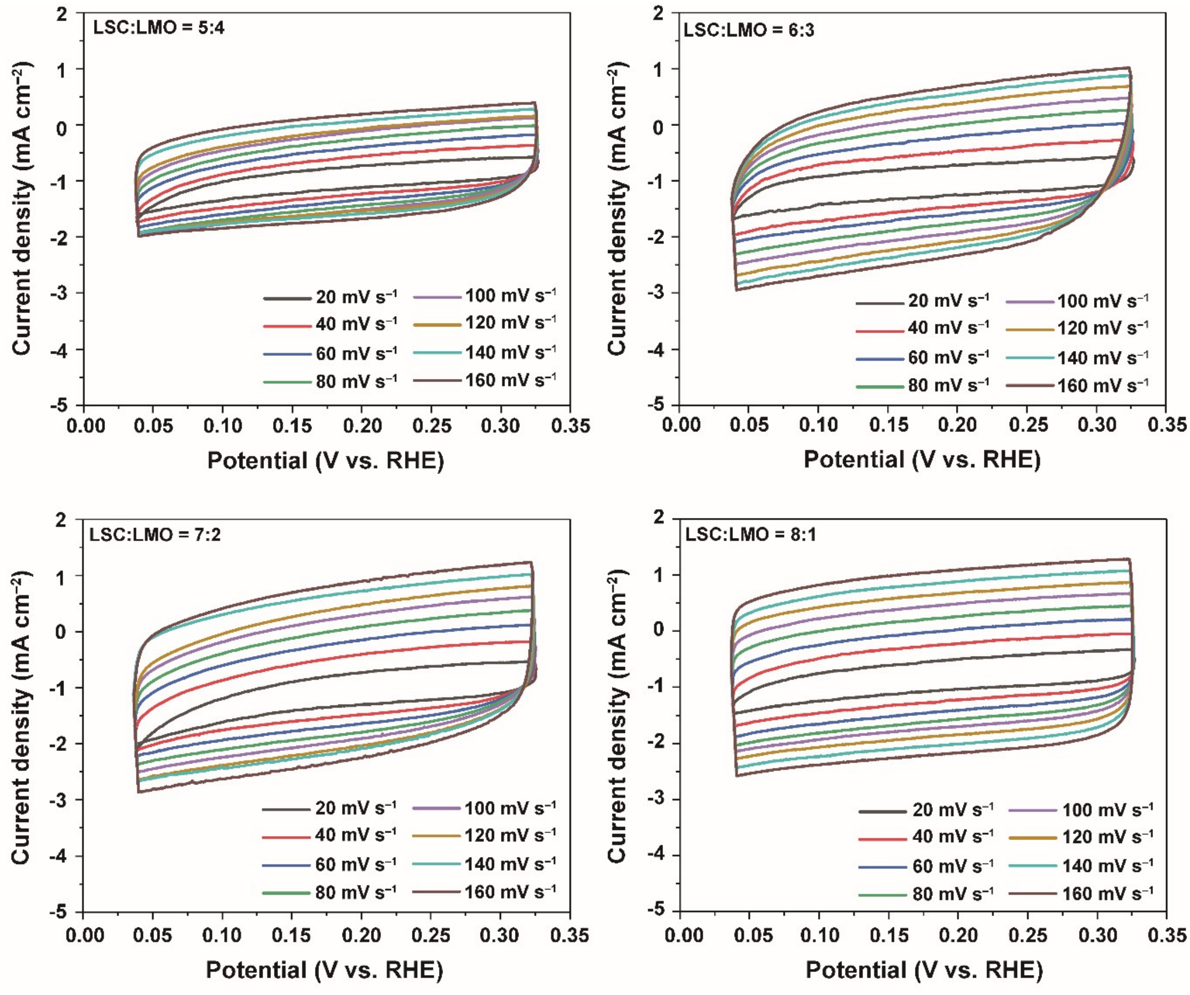

Fig. S4 Cyclic voltammetry (CV) curve of various weight ratios of LSC/LMO. Each CV curve in the double-layer capacitance region is measured at scan rates from 20 to 160 mV s^{-1} with a 20 mV s^{-1} interval.

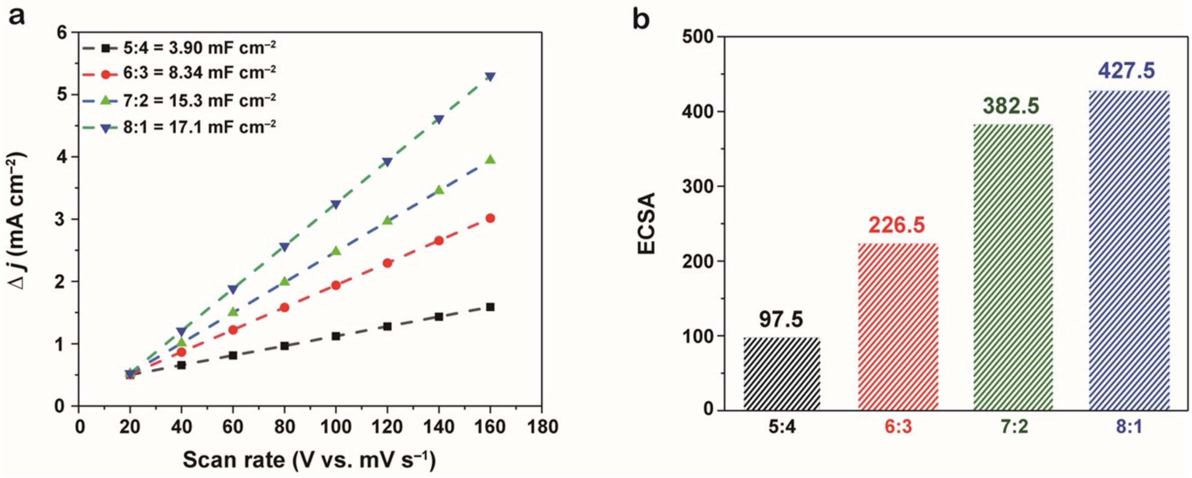

Fig. S5 (a) Double-layer capacitance values (C_{dl}) and (b) ECSA values of LSC/LMO with different weight ratios.

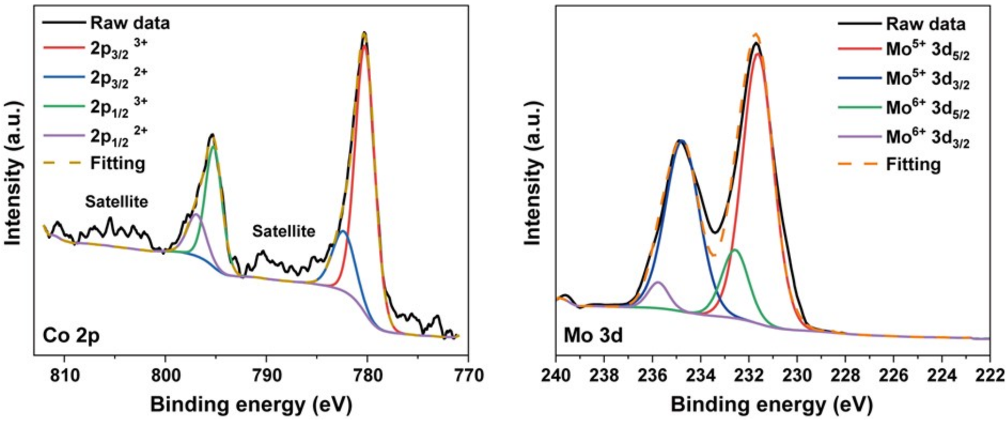

Fig. S6 High-resolution XPS spectra of Co 2p and Mo 3d of LSC/LMO after the chronoamperometric stability test at 100 mA cm^{-2} for 200 h.

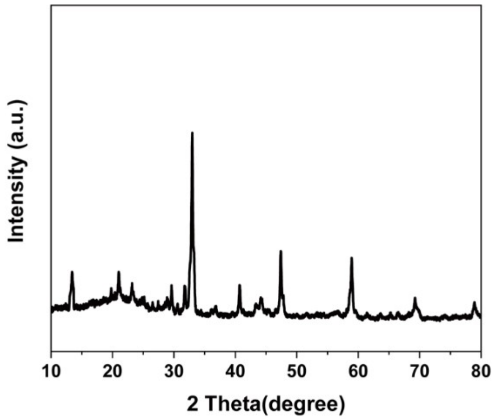

Fig. S7 XRD spectrum of LSC/LMO after the chronoamperometric stability test at 100 mA cm^{-2} for 200 h.

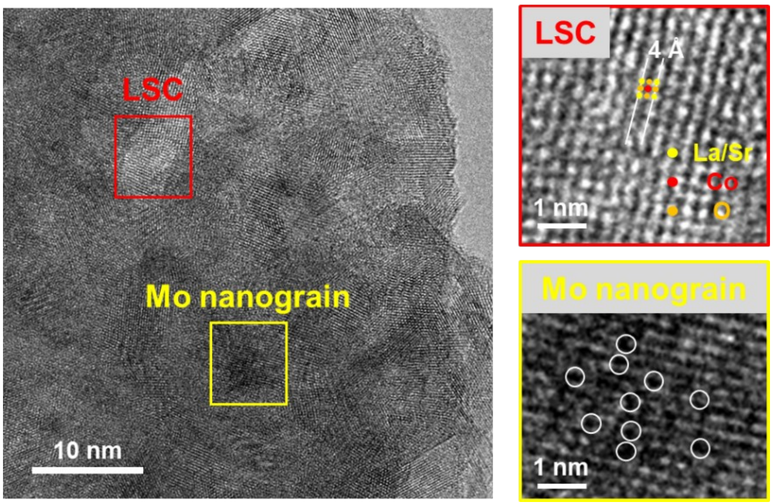

Fig. S8 TEM and HR-TEM images of LSC/LMO after the chronoamperometric stability test at 100 mA cm^{-2} for 200 h. Red and yellow boxes correspond to the domain of LSC and Mo nanograin, respectively.

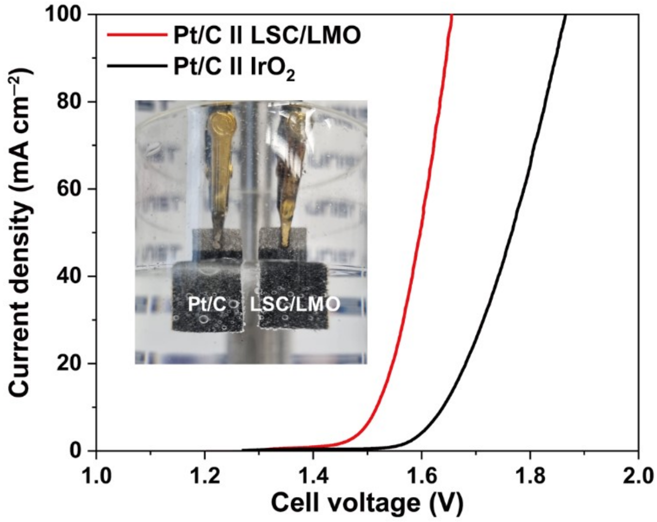

Fig. S9 Polarization curves for the overall water-splitting. The inset image shows the two electrodes system for the overall water-splitting.

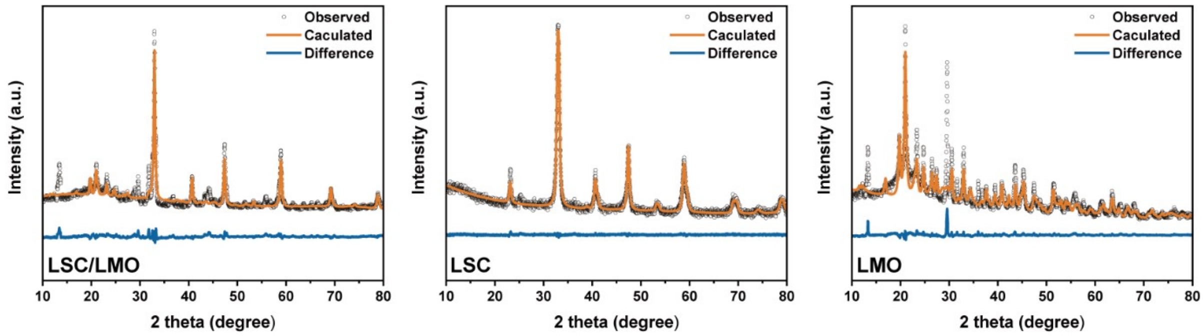

Fig. S10 Rietveld XRD refinement patterns of LSC/LMO, LSC, and LMO.

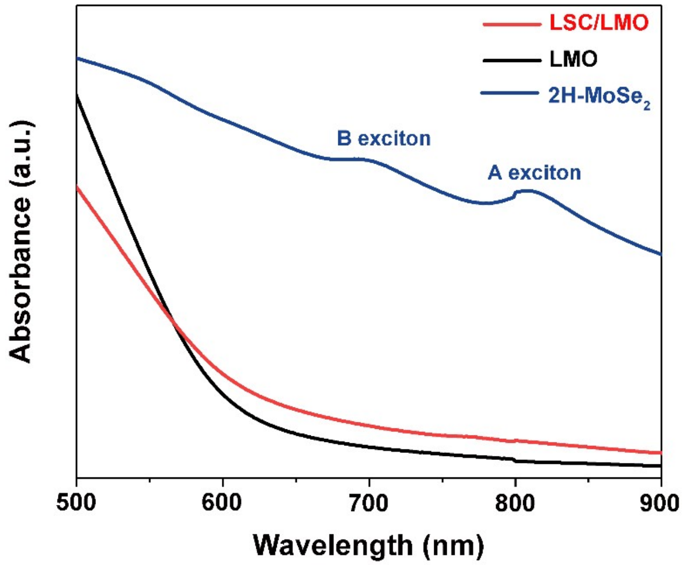

Fig. S11 UV–Vis–NIR spectra of LSC/LMO, LMO, and 2H-$MoSe_2$ indicating metallic features of LSC/LMO and LMO.

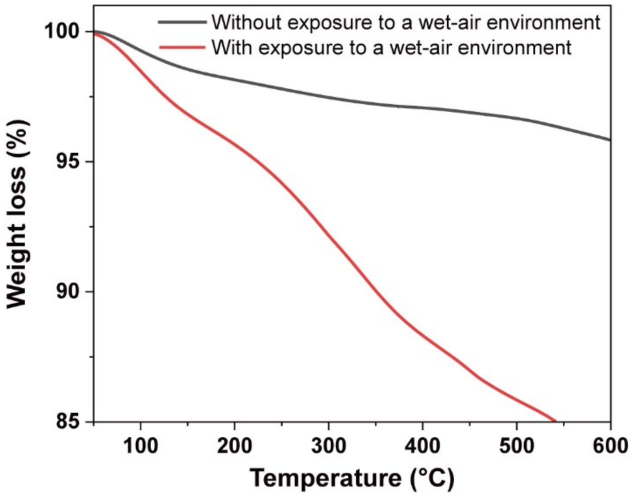

Fig. S12 TGA profile of LSC/LMO without and with exposure wet-air environment.

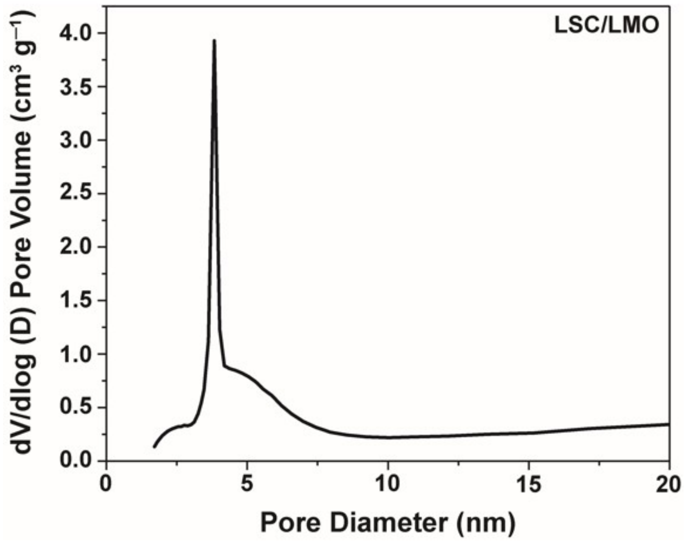

Fig. S13 Pore size distribution of LSC/LMO calculated from N_2 adsorption isotherms.

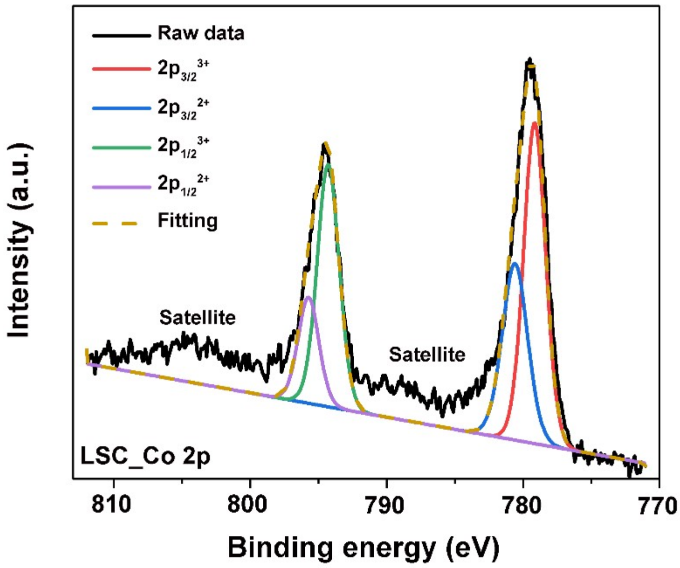

Fig. S14 High-resolution Co 2p XPS core-level spectrum for LSC.

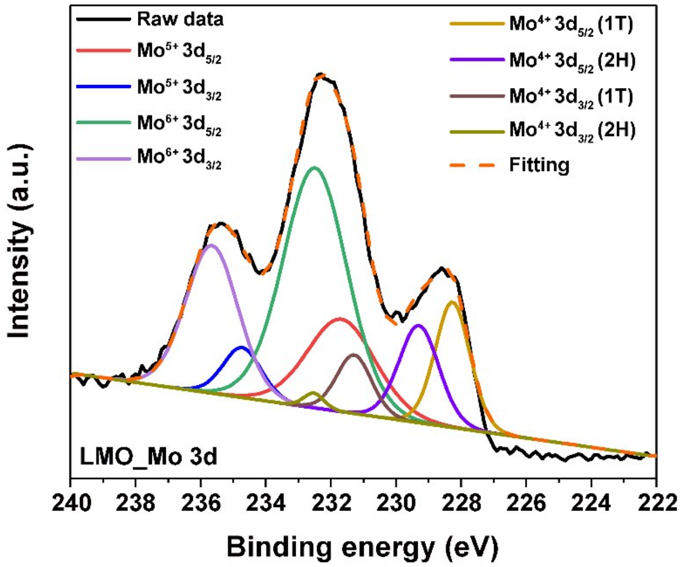

Fig. S15 High-resolution XPS spectrum of Mo 3d peak for LMO.

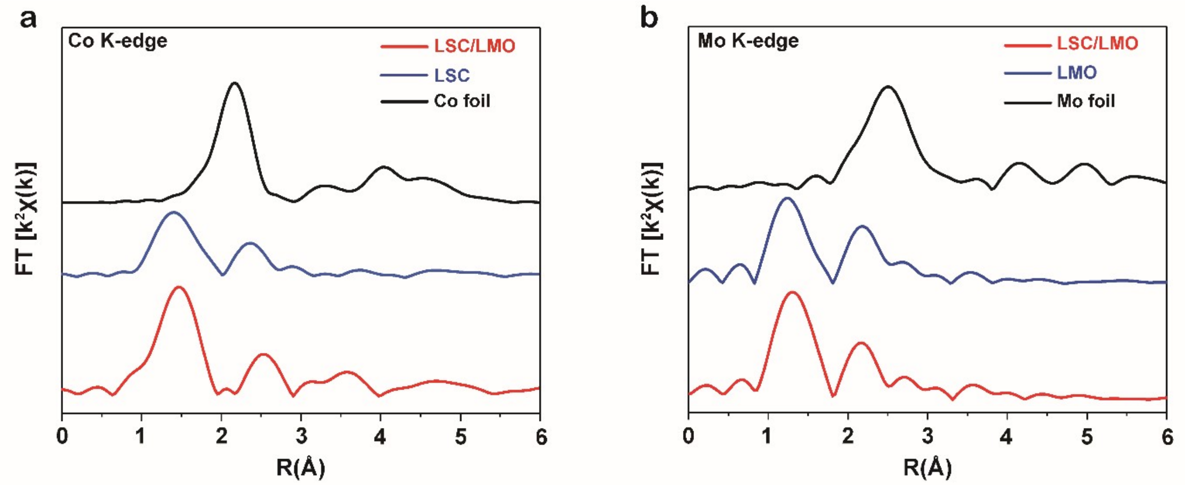

Fig. S16 Non-phase shifted Fourier transform (FT) EXAFS spectra of (a) Co K-edge of LSC/LMO, LSC, and Co foil and (b) Mo K-edge of LSC/LMO, LMO, and Mo foil.

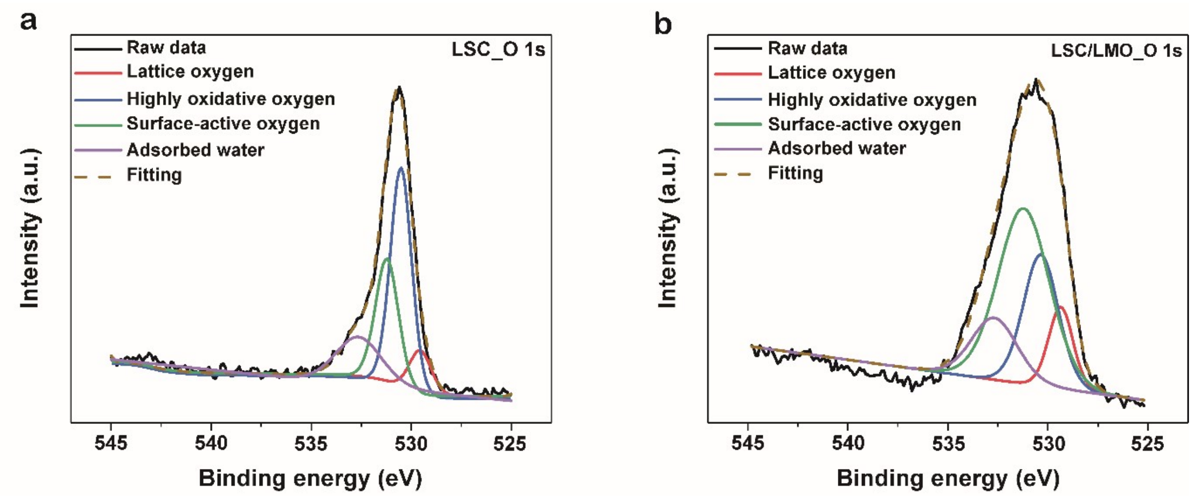

Fig. S17 High-resolution O 1s XPS core-level spectra for (a) LSC and (b) LSC/LMO.

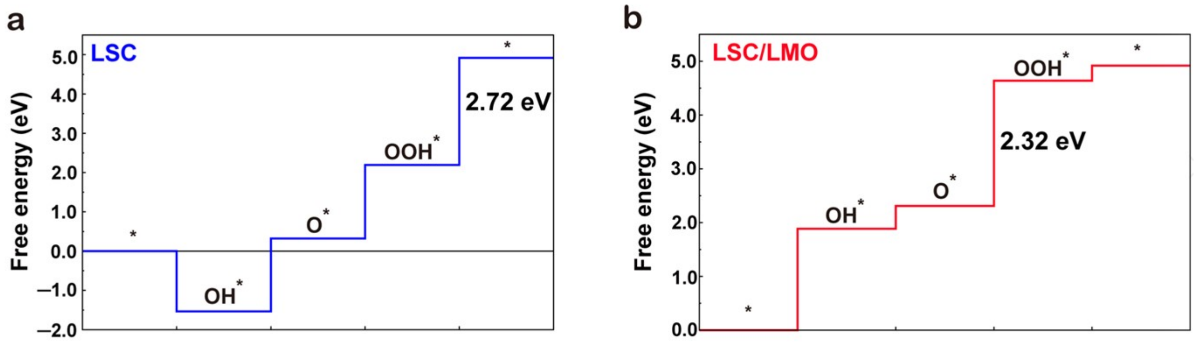

Fig. S18 Free energy diagrams for (a) LSC and (b) LSC/LMO in adsorbate evolution mechanism.

Table S1. Elemental composition of LSC/LMO determine by ICP-OES.

Element	Weight %	Atomic %
La	35.54	21.60
Sr	24.57	23.68
Co	35.46	50.81
Mo	4.43	3.91
Se	0.0	0.0
Total	100	100

Table S2. OER overpotential at 10 mA cm^{-2} of LSC/LMO with different weight ratios obtained from the OER polarization curve in Fig. S2.

Weight ratio	5:4	6:3	7:2	8:1	9:0	0:9
Overpotential at 10 mA cm^{-2} (V)	1.49	1.48	1.47	1.45	1.60	2.39

Table S3. Charge transfer resistance (R_{ct}) of LSC/LMO with various weight ratios obtained from the Nyquist plot analysis in Fig. S3.

Weight ratio	5:4	6:3	7:2	8:1
R_{ct} (Ω cm^2)	48.57	11.62	10.89	6.50

Table S4. Rietveld refined lattice parameters of LSC/LMO, LSC, and LMO.

Catalyst	Component	Proportion (wt%)	Space group	a (Å)	b (Å)	c (Å)
LSC/LMO	LSC	78.80	Pm3m	3.837	3.837	3.837
	Li_2MoO_4	27.20	R3	14.337	14.337	9.589
LSC	LSC	100	Pm3m	3.837	3.837	3.837
LMO	Li_2MoO_4	79.23	R3	14.337	14.337	9.589
	MoO_3	20.77	Pbnm	3.962	13.858	3.697

Table S5. Summary of the quantification of Co^{3+}/Co^{2+} ratios in LSC and LSC/LMO obtained from the XPS analysis in Fig. 3g and Fig. S14.

	LSC (atomic %)	**LSC/LMO (atomic %)**
Co $2p_{3/2}$, Co^{3+}	61.1	91.1
Co $2p_{3/2}$, Co^{2+}	38.9	8.9
Co^{3+}/Co^{2+}	ca. 1.6	ca. 10.3

Table S6. Summary of the quantification of Mo^{4+}, Mo^{5+}, and Mo^{6+} contents in LMO and LSC/LMO obtained from the XPS analysis in Fig. 3h and Fig. S15.

	LMO (atomic %)	LSC/LMO (atomic %)
Mo^{4+} $3d_{5/2}$ (1T)	10.5	2.4
Mo^{4+} $3d_{5/2}$ (2H)	9.3	
Mo^{4+} $3d_{3/2}$ (1T)	4.9	
Mo^{4+} $3d_{3/2}$ (2H)	0.7	
Mo^{5+} $3d_{5/2}$	14.9	48.6
Mo^{5+} $3d_{3/2}$	4.6	35.9
Mo^{6+} $3d_{5/2}$	36.6	11.1
Mo^{6+} $3d_{3/2}$	18.5	2.0
Total	100	100

Table S7. Summary of the quantification of lattice oxygen (AO), highly oxidative oxygen (BO), surface-active oxygen (CO), and adsorbed water (DO) in LSC and LSC/LMO obtained from the XPS analysis in Fig. S17.

	LSC (atomic %)	LSC/LMO (atomic %)
AO	10.1	10.9
BO	50.5	24.9
CO	28.3	48.9
DO	11.1	15.3
CO/AO	ca. 2.8	ca. 4.5

Table S8. Electrolyte resistance of tested catalysts obtained from the Nyquist plot in Fig. 2c.

Catalyst	R_s (Ω cm^2)
LSC/LMO	1.91
IrO_2	2.82
LSC	4.58
LMO	1.95

Note S1.

OER simulations

The Fig. 4c and Fig. S18 show a comparison between lattice oxygen participation mechanism (LOM) and adsorbate evolution mechanism (AEM) for OER free energies in the LSC and LSC/LMO systems. The LOM proceeds with elementary reactions below:

$$OH^{*} \rightarrow (V_O + OO)^{*} + H^{+} + e^{-}$$

$$(V_O + OO)^{*} + H_2O_{(l)} \rightarrow (V_O + OH)^{*} + O_{2(g)} + H^{+} + e^{-}$$

$$(V_O + OH)^{*} + H_2O_{(l)} \rightarrow (H_O + OH)^{*} + H^{+} + e^{-}$$

$$(H_O + OH)^{*} \rightarrow OH^{*} + H^{+} + e^{-}$$

, where OH, V_O, OO, and H_O indicate OH adsorbates, oxygen vacancies, OO adsorbates, and hydrogen atoms adsorbed on lattice oxygen, respectively. * represents that the adsorbates are bound to the LSC (001) surface.

The AEM proceeds with elementary reactions below:

$$^{*} + H_2O_{(l)} \rightarrow OH^{*} + H^{+} + e^{-}$$

$$OH^{*} \rightarrow O^{*} + H^{+} + e^{-}$$

$$O^{*} + H_2O_{(l)} \rightarrow OOH^{*} + H^{+} + e^{-}$$

$$OOH^{*} \rightarrow {}^{*} + O_{2(g)} + H^{+} + e^{-}$$

, where OOH indicates OOH adsorbates.